mater.scichina.com link.springer.com

Published online 19 August 2021 | https://doi.org/10.1007/s40843-021-1745-5
Sci China Mater 2022, 65(2): 442–450

UV soaking for enhancing the photocurrent and response speed of $Cs_2AgBiBr_6$-based all-inorganic perovskite photodetectors

Ye Yuan[1,2], Genghua Yan[1,2*], Zhuowei Li[2], Bangqi Jiang[2], Zongcun Liang[1], Hong Jin Fan[4] and Wenjie Mai[2,3*]

ABSTRACT **The response speed of the reported $Cs_2AgBiBr_6$-based photodetectors exhibits a wide variation ranging from microseconds to nanoseconds, while the reason is still unclear. Apart from the conventional approaches such as reducing effective area, new regulating approaches for response speed improvement have rarely been reported. On the other hand, it is generally believed that ultraviolet (UV) light has negative impact on perovskite devices resulting in performance degradation. In this work, we demonstrated that the response speed of the photodetector with FTO/$Cs_2AgBiBr_6$/Au structure can be effectively regulated by utilizing UV light-soaking effect without reducing the device area. Particularly, the decay time is efficiently modulated from 30.1 μs to 340 ns. In addition, the −3 dB bandwidth of the device is extended from 5 to 20 kHz. It is worth mentioning that the light current is remarkably boosted by 15 times instead of any attenuation. Furthermore, we prove the universality of UV soaking treatment on $Cs_2AgBiBr_6$-based photodetectors with other all-inorganic structures, i.e., FTO/TiO_2/$Cs_2AgBiBr_6$/Au, FTO/$Cs_2AgBiBr_6$/TiO_2/Au and FTO/TiO_2/$Cs_2AgBiBr_6$/CuSCN/Au. Our results demonstrate a new method to improve the response speed and light current of $Cs_2AgBiBr_6$-based perovskite all-inorganic photodetectors.**

Keywords: UV light, all-inorganic perovskite photodetectors, $Cs_2AgBiBr_6$, photocurrent, response speed

INTRODUCTION

Perovskite materials are one of the most sparkly stars in the optoelectronic field within the last decade owing to their outstanding photoelectric features, including high light absorption coefficient, large carrier mobility, long charge diffusion length and tunable bandgaps [1–4]. To date, various kinds of perovskite materials have been widely applied for optoelectronic devices, such as solar cells [5,6], light emitting diodes [7,8] and photodetectors [9–11], showing attractive prospects for both academic and industrial communities. However, some challenges still remain regardless of the rapid increase of device performance. Among them, the ultraviolet (UV) stability and the light-soaking effect are issues that have received significant attention and investigation. In general, UV light is considered as an adverse factor for perovskite-based devices, especially for the organic-inorganic hybrid perovskite species, as it would result in the decomposition of perovskite materials [12,13]. In this case, developing all-inorganic perovskite materials is a promising strategy to overcome the issue of UV stability. Chen and co-workers [14] used a synergistic effect of gradient thermal annealing and anti-solvent to precisely control the growth of α-$CsPbI_2Br$ crystals and the power conversion efficiency (PCE) of the corresponding solar cell maintained 90% of the initial one after aging for 120 h under 100 mW cm^{-2} UV irradiation. Wang's group [15] combined a solution-phase process and halide exchange technology to prepare $CsPbBr_3$ nanowire films and fabricated the corresponding photodetectors with metal-semiconductor-metal structure, which showed outstanding stability under UV light (5 V, 2.7 mW cm^{-2}) for more than 10,000 s. On the other hand, light-soaking effect, which depicts the increasing device performance upon continuous light illumination, has strongly impact on the long-term operational stability of the devices. Some promising approaches have been reported to reduce or eliminate the instability, leading to highly stable perovskite devices. Wang *et al.* [16] employed n-type organic molecules as modification materials between the electron-transport-layer (ETL) and perovskite layer to eliminate the light-soaking effect in solar cells. Liu's group [17] successfully fabricated γ-$CsPbI_3$ films and further optimized them by doping chlorine ions, the device of which showed only 0.45% degradation after continuous light soaking for 200 h.

It is noteworthy that the optimizing avenues should be consistent with the actual application requirements of the devices. On this occasion, the optimizing avenues for solar cells may not be suitable for photodetectors. Moving forward, the negative effect on solar cells could be a positive one on photodetectors. As mentioned above, the performance of the perovskite-based devices would show an increasing tendency under continuous light illumination, which is so called light-soaking effect. In the field of solar cells, light-soaking effect is considered as one type of instability and hinders the precise evaluation of device performance, which has been eliminated by several approaches.

[1] Institute for Solar Energy Systems, Guangdong Provincial Key Laboratory of Photovoltaic Technology, School of Physics, Sun Yat-sen University, Guangzhou 510006, China
[2] Siyuan Laboratory, Guangdong Provincial Engineering Technology Research Center of Vacuum Coating Technologies and New Energy Materials, Department of Physics, Jinan University, Guangzhou 510632, China
[3] Guangdong Provincial Key Laboratory of Optical Fiber Sensing and Communications, Jinan University, Guangzhou 510632, China
[4] School of Physical and Mathematical Sciences, Nanyang Technological University, Singapore 637371, Singapore
* Corresponding authors (emails: yangh373@mail.sysu.edu.cn (Yan G); wenjiemai@email.jnu.edu.cn (Mai W))

However, why not consider another point of view? It is possible to desire that the light-soaking effect could be a promising strategy to improve the photoresponse performance of photodetectors.

Furthermore, response speed is a significant parameter to evaluate the performance of photodetectors, representing the ability of a photodetector to track rapidly changing incident light signals [18]. For example, in an optical communication system, the response speed of a photodetector highly determines the information rate. In general, the response speed could be improved by reducing the device area and modifying the device structure. For inorganic perovskite-based photodetectors, the reported response show a wide distribution. In 2018, Lei *et al.* [19] first reported a $Cs_2AgBiBr_6$ photodetector and obtained a response speed of 956/995 μs. Chi and co-workers [20] synthesized Cs_3BiBr_6 crystals and fabricated the photodetector with a response speed of 50/60 ms. Tang's group [21] demonstrated a response speed of ~1 ms with $Cs_2AgBiCl_6$ single crystal. Besides, even though the structure is similar, widely different response speeds have been reported. Wu *et al.* [22] prepared a photodetector with the structure of SnO_2/$Cs_2AgBiBr_6$, which presented a response speed of ~2 ms. Gao's group [23] fabricated a SnO_2/$Cs_2AgBiBr_6$/TFB structured photodetector and enhanced the response speed from 374 to 17 ns by minimizing the active area from 7.25 to 0.2 mm^2. We observe that the response speed of all-inorganic perovskite-based photodetectors exhibits randomness at some extent, for which the reason is not clear. What is more, the investigation on new-type approach for response speed regulation has been barely reported.

Light-soaking effect is a pervasive phenomenon for perovskite-based devices, which would result in a hysteresis effect and weakened the device stability, therefore harmful to the device performance. Nevertheless, the reason for the light-soaking effect still has not reached a consensus in the community. Moreover, it is found that several optical processing approaches have been adopted for device performance improvement in the perovskite optoelectronic field. Niezgoda and co-workers [24] investigated the performance evolution of $CsPbBrI_2$ solar cells under continuous illumination (AM1.5). The devices exhibited dramatic performance enhancement, resulting from the light-induced dealloying of $CsPbBrI_2$ that improved the collection of holes. Xue *et al.* [25] raised an approach that used the above-bandgap illumination with a small energy threshold (1.6 mW cm^{-2}) to trigger reversible phase transition from orthorhombic to tetragonal in $CsPbBr_3$, which presented a fast and controllable response to light on/off. They demonstrated that such photon-induced dynamic structure reorganization was caused by the transition of torsion direction in Pb-Br octahedral, while the diffusion potential difference induced by local Coulombic field was proved to drive this process. Yan's group [26] utilized a laser-annealing method to obtain high-crystallinity perovskite films, benefiting from the laser-induced high temperature gradient and in consequence leading to the selective growth of large perovskite grains. Hence, it is worth expecting that the simple optical processing approach could be effective for new-type perovskite performance improvement.

Herein, we find that the reasonable use of UV light-soaking effect could be beneficial to the perovskite devices. Thus, we report an innovative UV-induced method to efficiently regulate the response speed of the $Cs_2AgBiBr_6$-based all-inorganic perovskite photodetectors (free of organic hole transport layer and ETL). We demonstrated the favorable UV stability of $Cs_2AgBiBr_6$ films and photodetectors with appropriate modification in our previous work [27]. Based on it, in this work, we fabricated all-inorganic $Cs_2AgBiBr_6$-based photodetectors and investigated the effect of UV illumination on the photoresponse performance. Satisfyingly, it is found that the rise/decay edge of photoresponse curves can be effectively modified by UV illumination, taking advantage of the light-soaking effect, which results in the remarkable improvement of response speed. To be specific, the response speed of the photodetector with the structure of fluorine-doped tin oxide (FTO)/$Cs_2AgBiBr_6$/Au is successfully regulated from 30.1 μs to 340 ns without reducing the device area. In addition, the light current of the $Cs_2AgBiBr_6$ photodetector exhibits evident increase with UV soaking treatment as well, which is significantly boosted from ~1.0×10^{-5} A to ~1.5×10^{-4} A. Furthermore, we demonstrate the universality of the UV soaking treatment method for $Cs_2AgBiBr_6$-based all-inorganic photodetectors with different structures. According to the characterization results, the increased light current and enhanced response speed could be attributed to the improved electrical properties of the devices after UV treatment. Our work provides a fresh perspective on the improvement of the $Cs_2AgBiBr_6$-based all-inorganic photodetectors.

EXPERIMENTAL SECTION

Preparation of the $Cs_2AgBiBr_6$-based photodetector

Firstly, FTO glass substrates were ultrasonically cleaned in isopropyl alcohol, deionized water, and ethyl alcohol for 15 min, successively. For the $Cs_2AgBiBr_6$ precursor solution, 212.8 mg of CsBr powders, 93.9 mg of AgBr powders, and 224.4 mg of $BiBr_3$ powders were added in dimethylsulfoxide (DMSO) with a concentration of 0.5 mol L^{-1}. The mixture was heated to 80°C and continuously stirred until the powders were totally dissolved. $Cs_2AgBiBr_6$ thin films were prepared by a one-step spin-coating method. Prior to spin-coating, cleaned substrates were blown by high-purity N_2 stream and treated by UV-ozone for 15 min. Both the substrates and the solution were preheated to 80°C. During the process, the precursor solution was spin-coated onto the substrates at 500 rpm for 6 s and then at 3000 rpm for 50 s. Then, the coated samples were annealed at 285°C for 5 min. The whole process of $Cs_2AgBiBr_6$ thin film preparation was performed in a N_2-filled glove box. The TiO_2 layers were prepared by an atomic layer deposition (ALD) process. During the process, titanium tetrachloride ($TiCl_4$), H_2O vapor and high-purity N_2 were used as the precursor, reactant and carrier gas, respectively. Meanwhile, the temperature was fixed at 105°C while the thickness of TiO_2 layer was controlled to be 15 nm. For the preparation of CuSCN layers, a spin-coating process along with a fast solvent removal method was carried out. The CuSCN precursor solution was produced by dissolving 60 mg of CuSCN powders (Kanto Chemical Co., Inc, 99.5% purity) into 1 mL of diethyl sulfide (Macklin, ≥98% purity) after stirring for half an hour at room temperature. During the spin-coating process, the rate and time were fixed at 7000 rpm and 50 s, respectively. Specially, the CuSCN precursor solution was spin-coated on the substrates quickly when the rate was stable. Then, the coated samples were annealed at 100°C for 5 min. Finally, 80-nm gold layers were deposited by thermal evaporation at a pressure of 8×10^{-4} Pa through a shadow mask. The effective area of illumination for all

the devices is 0.0157 cm^2, while the area of heterojunction is ~1.9 cm^2.

UV treatment of the $Cs_2AgBiBr_6$-based photodetector

A xenon lamp was used as the light source for UV treatment (365 nm, 250 W). The $Cs_2AgBiBr_6$ photodetector samples were placed in front of the xenon lamp. The illumination time was fixed at 1, 3, 5, 8 h, respectively. The process of UV treatment was carried out in a fuming cupboard to avoid the destructive effect of ozone. After UV illumination, all of the samples were placed in ambient for a period of time before the subsequent measurements, in order to avoid the thermal effect of UV light.

Materials and device characterization

X-ray diffraction (XRD) was used to identify the crystal structure with Cu Kα1 radiation (λ = 1.54056 Å) from 10° to 50°. The surface morphology of the $Cs_2AgBiBr_6$ films were characterized by scanning electron microscope (SEM, Zeiss Sigma 300), which was combined with an energy-dispersive X-ray spectroscopy (EDS) system (Bruker XFlash6) for composition analysis. The electrochemical impedance spectra (EIS) were conducted by a Princeton electrochemical workstation (Veras STAT 3-400). The measured frequencies ranged from 0.1 Hz to 1 MHz with varying bias from 0 to 0.6 V. The amplitude was 20 mV. For device performance, a homemade measurement system combining a laser diode (405 nm), an oscilloscope, a pulse generator and a Keithley 2400 source meter was used to investigate the photoresponse performance. The response was evaluated by a waveform generator and a digital oscilloscope (Tektronix TDS 2012C).

RESULTS AND DISCUSSION

UV-induced performance improvement of the $Cs_2AgBiBr_6$-based photodetectors

The schematic of the photodetector is presented in Fig. 1a, which illustrates the structure of FTO/$Cs_2AgBiBr_6$/Au. Fig. 1b shows the photoresponse curves of the $Cs_2AgBiBr_6$-based devices under different UV-treatment time with the illumination of 1 W cm^{-2} (405 nm, 0 V). Evidently, the light current (I_{light}) of the devices presents an increasing tendency with prolonged UV illumination. It is boosted from ~1.0×10^{-5} to ~1.5×10^{-4} A after UV treatment for 8 h, showing a 15-fold improvement. Fig. 2a displays the specific variation of I_{light} and dark current (I_{dark}) along with the UV-treatment time. The I_{light} shows a sharply rising trend first and then rises slowly with the increase of UV-treatment time, which is believed to tend to be saturated after UV illumination for 3 h. Besides, as for the I_{dark}, it exhibits a slightly upward trend. Accordingly, the on-off ratio rises from 4.4×10^2 to the maximum value of 5.7×10^3 after UV illumination for 1 h. In addition, the responsivity (R), which is calculated by $R = I/P$, where I and P represent the photogenerated current and light power intensity, respectively, increases from 0.7 to 9.8 mA W^{-1} after 8 h of UV illumination. Likewise, the detectivity (D^*), another key performance evaluation index for photodetectors, is boosted nearly an order of magnitude after UV treatment, as is shown in Fig. S1. Meanwhile, the noise level of the measurement system is shown in Fig. S2. More importantly, the rising and falling edges of the photoresponse curves can be effectively regulated by controlling the UV treatment time, as shown in Fig. 1c–f. It is observed that the curve shape of I_{light} trends from slash to flatline (Fig. 1c, d). Besides, the variation of I_{dark} exhibits the same tendency, which is obtained by taking the logarithm of the curves (Fig. 1e, f). What needs to be clarified is that the presented outliers in Fig. 1e would disappear when measured under high frequencies (Fig. S3). Therefore, the outliers have little impact on the high-frequency performance of the device. It is known that the rise and decay times of a photodetector are identified from the time interval for the response to rise (decay) from 10% (90%) to 90% (10%) of its peak value [28]. Hence, the rising and falling edges highly determine the response speed of photodetectors. This indicates that the UV-

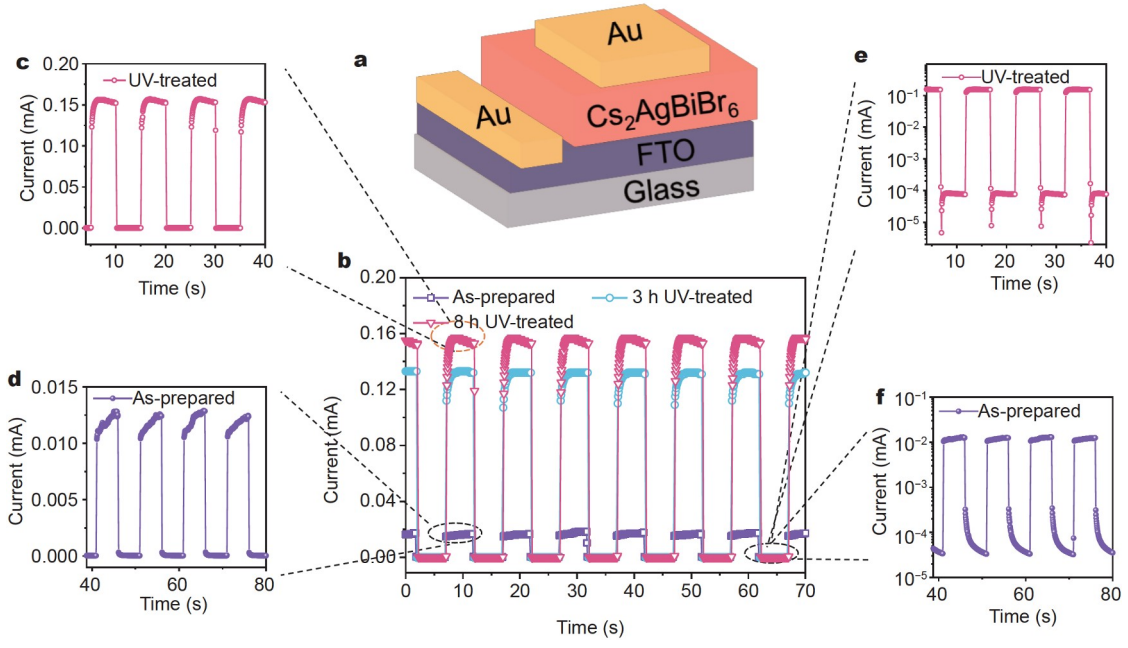

Figure 1 (a) Structure diagram of the $Cs_2AgBiBr_6$ photodetector. (b) *I-T* curves of the as-prepared device and the device with UV treatment. (c–f) Enlarged *I-T* curves of the corresponding devices.

induced regulation could significantly improve the response of the $Cs_2AgBiBr_6$ perovskite photodetectors, which will be discussed later. The current-voltage (*I-V*) characteristics of the as-prepared and UV-treated (8 h) photodetectors are shown in Fig. S4. It clearly demonstrates the self-powered property of the devices. In Fig. 2b, the spectral photoresponse performances of the $Cs_2AgBiBr_6$ devices are presented. Obviously, the responsivity of the UV-treated device exhibits distinct improvement in the whole range, benefiting from the increase of I_{light}. Besides, the linear dynamic range (LDR) of the devices is calculated to be 60 and 87 dB, respectively, as shown in Fig. S5.

The normalized photoresponse to incident pulse laser frequency was analyzed and determined by −3 dB bandwidth, which represents the ability of high-frequency response. Fig. 2c exhibits the results of the as-prepared and UV-treated devices. It can be seen that the −3 dB bandwidth increases from ~5 to ~200 kHz with 5 h of UV soaking treatment. Fig. 2d presents the enlarged temporal photoresponse curves of the samples measured under −3 dB frequency. The rise/decay times of the as-prepared, 3-h UV-treated and 5-h UV-treated devices are determined to be 55.9/30.1 μs, 26.3/1.3 μs and 1.1/0.34 μs, respectively. This indicates that the response speed of the $Cs_2AgBiBr_6$ perovskite photodetectors can be effectively regulated by controlling the time for UV exposure. The detailed −3 dB bandwidths and responses of the devices UV-treated for 0 to 8 h are listed in Table 1. Though the −3 dB bandwidth shows slight decline for the 8 h UV-treated sample, the corresponding response speed still remains at a favorable level (1.2/0.51 μs). It is hard to avoid the effect of ozone which is generated under long-time UV illumination on the device performance. The details will be discussed later.

To investigate the UV stability of the $Cs_2AgBiBr_6$ perovskite films, the pre- and post-treatment properties of morphology, component distribution and phase structure were characterized. As shown in Fig. 3a, b, the surface morphologies of the as-prepared and UV-treated $Cs_2AgBiBr_6$ films exhibit little difference, with similar average grain size of ~350 nm. Likewise, no obvious halide ion migration or phase segregation are observed in the element mappings of the two films, as shown in Fig. S6. All the elements of the samples are evenly distributed. Besides, Fig. 3c displays the XRD patterns of the $Cs_2AgBiBr_6$ devices before and after UV illumination for 3 h. It is found that both of the samples have diffraction peaks located at 13.63°, 15.73°, 22.32°, 27.41°, 31.75°, 35.63°, 39.15° and 45.51°, which could be assigned to the (111), (002), (022), (222), (004), (024), (224) and (044) planes of crystalline $Cs_2AgBiBr_6$ films, suggesting the formation of cubic perovskite structure (space group *Fm*3*m*, *a* = 11.2640 Å) [29]. Whereas, the peaks at 38.23° and 44.41° could be assigned to Au electrode while those at 26.49°, 33.68° and 37.72° could be ascribed to the FTO substrates. Evidently, there is no phase change of the perovskite films after UV illumination treatment. These results further reveal the favorable UV stability

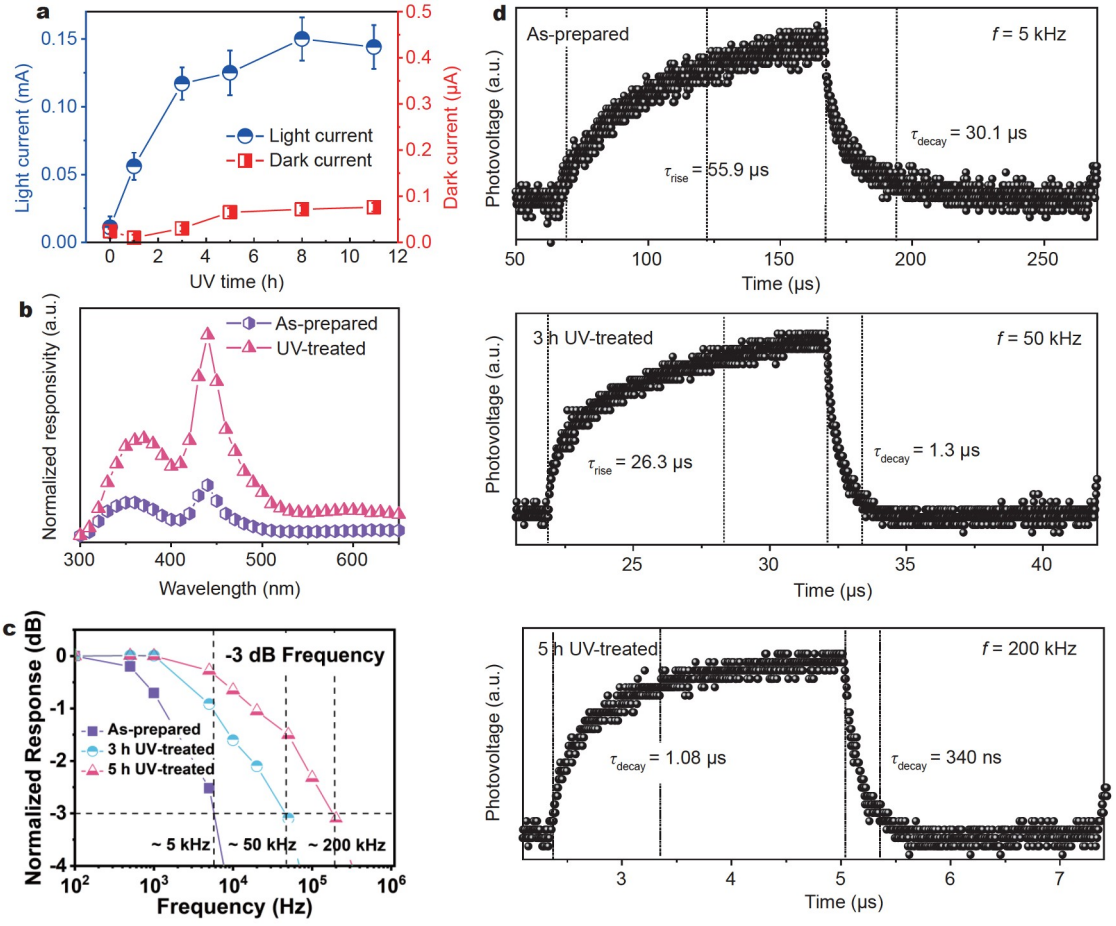

Figure 2 The influence of the UV soaking treatment on (a) light current and dark current, (b) spectral photoresponse performance, (c) −3 dB bandwidth and (d) response speed of the devices.

Table 1 The detailed results of −3 dB bandwidth, rise time and decay time of the devices with different UV soaking times

UV time (h)	0	1	3	5	8
−3 dB bandwidth (kHz)	~5	~10	~50	~200	~100
Rise time (μs)	55.9	39	26.3	1.08	1.2
Decay time (μs)	30.1	11	1.3	0.34	0.51

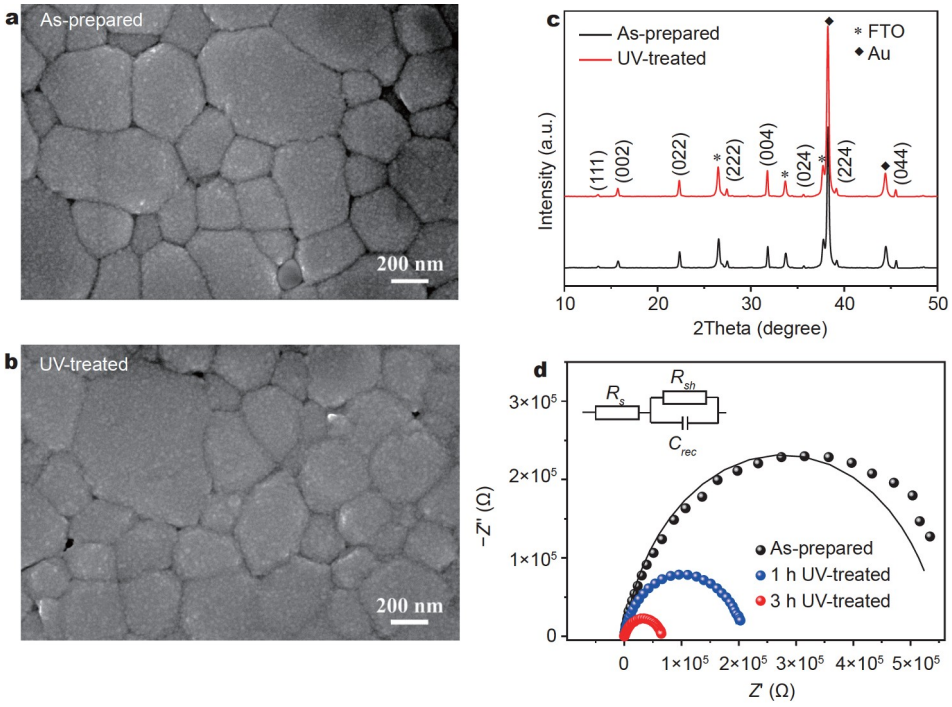

Figure 3 SEM images of (a) the as-prepared and (b) UV-treated $Cs_2AgBiBr_6$ films at high magnification. (c) XRD patterns of the as-prepared and UV-treated devices. (d) EIS spectra of the devices without and with different UV soaking times. The inset is the equivalent circuit.

of the $Cs_2AgBiBr_6$ films.

Afterwards, EIS were carried out to investigate the electrical property of the devices. Fig. 3d shows the Nyquist plots for the FTO/$Cs_2AgBiBr_6$/Au device after different UV illumination times. The inset presents the diagram of equivalent circuit used for fitting, where R_s is the series resistance, R_{sh} and $C1$ is the resistance and capacitance of the bulk $Cs_2AgBiBr_6$ layer, respectively. Table S1 lists the fitting results of R_s. In general, the response speed is mainly determined by the series resistance of the device. It is found that the series resistance of the $Cs_2AgBiBr_6$ photodetector shows an evident decreasing trend from 85.52 to 40.02 Ω with 3 h UV soaking, resulting in the improvement of the response speed. In addition, according to the formula: $R_{res} \propto (n \times \mu)^{-1}$, where n and μ is the carrier concentration and mobility, respectively, it is reasonable to speculate that the carrier concentration and/or mobility of the device tend to increase with UV illumination. The underlying mechanism of the light-soaking effect has received much attention, which still has no unified understanding in the perovskite community. To date, some possible reasons have been reported in the literatures, including ion migration [30–32], interface charge trapping/detrapping [33,34], defect compensation [35–39] and phase segregation [40,41]. According to the above analyses of EIS and resistance, the reason for the improved I_{light} of our devices could be attributed to the defect compensation in the bulk and interface during UV soaking, leading to the increase of carrier concentration and/or mobility. We perform the space-charge-limited-current (SCLC) analysis to evaluate the defect level of the photodetectors without and with UV treatment, as shown in Fig. S7. There are three transition regions in the SCLC curve, i.e., linear Ohmic, trap-filled limit (TFL) and trap-free Child. In the TFL region, all defect traps are filled [42]. The onset voltage of TFL region (V_{TFL}) can be used to determine the defect density N by the following expression [42]

$$N = \frac{2\varepsilon\varepsilon_0}{ed^2}V_{TFL}, \quad (1)$$

where $\varepsilon_0 = 8.85 \times 10^{-12}$ pF m^{-1} is the vacuum permittivity [43], ε is the static dielectric constant which is taken as 16.73 for $Cs_2AgBiBr_6$ [42], e is the the charge quantity and d is the film thickness. In consequence, the defect density of the device without and with UV treatment is calculated to be 8.97×10^{16} and 3.33×10^{16} cm^{-3}, respectively. The decrease of defect density after UV illumination further demonstrates our speculation for the improvement of I_{light} and response speed, which is consistent with the EIS analysis.

Furthermore, we investigated the aging stability of the $Cs_2AgBiBr_6$ photodetectors after UV illumination. Note that the devices with 8 h UV treatment were used for aging test. During

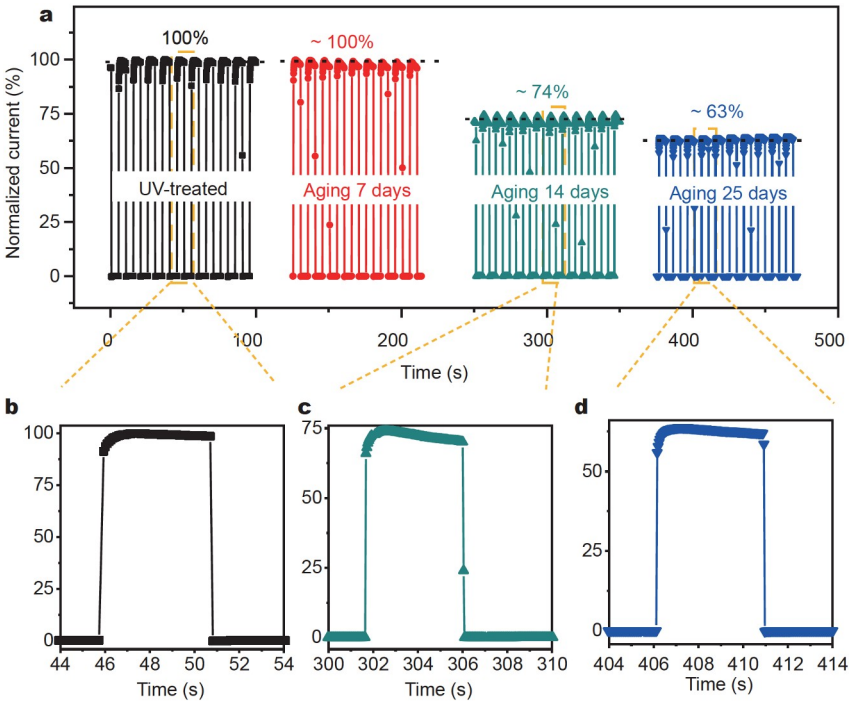

Figure 4 (a) The aging stability of the $Cs_2AgBiBr_6$ photodetector after UV soaking treatment. No illumination was performed during aging test. (b–d) Enlarged *I-T* curves of the device with different aging times.

the test, the devices were stored in a constant-humidity cabinet with 10% RH and without further illumination. Fig. 4 reveals the photoresponse curves of the device with different aging times after UV treatment. It is found that the I_{light} of the device remains stable after aging for 7 days, which demonstrates the favorable stability of the $Cs_2AgBiBr_6$ photodetector and the durable effect of the UV illumination treatment. Subsequently, the I_{light} exhibits a declining tendency. When aging for 25 days, the I_{light} remains 63% of its original value. Whereas, according to the enlarged photoresponse curves shown in Fig. 3b–d, the UV-induced ultrafast photoresponse speed of the $Cs_2AgBiBr_6$ photodetector still exists rather than falling back to the initial one (like in Fig. 1d).

Investigation on the universality of UV soaking treatment

We realized that some details may lead to the deterioration of the device performance during the process of UV soaking. One is the electrode materials. As seen in Fig. S8a, b, the Ag electrodes would be oxidized and turn black after UV soaking, which is disadvantageous for the device performance. Nevertheless, the Au electrodes could keep the original state after UV illumination. In addition, the ventilation environment is also an important factor for the process. When the sample was placed in a poorly ventilated environment, the perovskite layer would be damaged by the ozone generated by the UV light, as shown in Fig. S8c.

In this section, $Cs_2AgBiBr_6$-based photodetectors with other structures were fabricated as well to investigate the universality of the approach of UV-induced regulation for photoresponse performance improvement. To be specific, photodetectors with structures of FTO/$Cs_2AgBiBr_6$/TiO_2/Au, FTO/TiO_2/$Cs_2AgBiBr_6$/Au and FTO/TiO_2/$Cs_2AgBiBr_6$/CuSCN/Au were prepared separately. It is worth mentioning that the conventional TiO_2 layers prepared by the spin-coating process would decompose the $Cs_2AgBiBr_6$ perovskite film during UV illumination, as seen in Fig. S8d. In this case, all of the TiO_2 layers were prepared by the ALD process. In our previous work, we demonstrated that compared with spin-coated TiO_2 layers, the photocatalytic activity of the ALD-TiO_2 layers is much lower, resulting in the satisfying stability of the perovskite device under the process of UV soaking [27]. Fig. 5 displays the photoresponse performance of the as-prepared and UV-treated photodetectors with the structure of FTO/$Cs_2AgBiBr_6$/TiO_2/Au. It is observed that the I_{light} of the photodetector is remarkably boosted from ~1×10^{-4} to ~5×10^{-4} A after UV treatment for 3 h, while the on-off ratio increases from ~9×10^4 to ~7×10^5 as well. In consequence, the *R* and D^* increase from 7.13 mA W^{-1} and 4.56×10^{10} Jones to 32.5 mA W^{-1} and 2.72×10^{11} Jones after UV illumination. Meanwhile, the peak intensity of the spectral photoreponse is obviously enhanced after UV treatment, as shown in Fig. 5b. From the enlarged temporal photoresponse curves shown in Fig. 5c, it is found that the response speed of the device is speeded up from 2.18 ms to 540 μs under the frequency of 100 Hz. Moreover, the *I-V* curves presented in Fig. S9 exhibit an increase in the open-circuit voltage after UV treatment.

With regard to the devices with the structures of FTO/TiO_2/$Cs_2AgBiBr_6$/Au and FTO/TiO_2/$Cs_2AgBiBr_6$/CuSCN/Au, similar results were obtained. The performance evaluation indices, including I_{light}, *R*, D^*, response speed and open-circuit voltage present increasing trends after the UV soaking treatment. Additionally, the spectral responsivity of the UV-treated photodetector shows obvious enhancement in the whole range (350–500 nm). The corresponding results can be found in Table S2 and Figs S10–S13. In addition, EIS and R_s of these three devices are presented in Figs S14–S16 and Table S1. Similar to the above results, the series resistance of all three devices exhibit decreas-

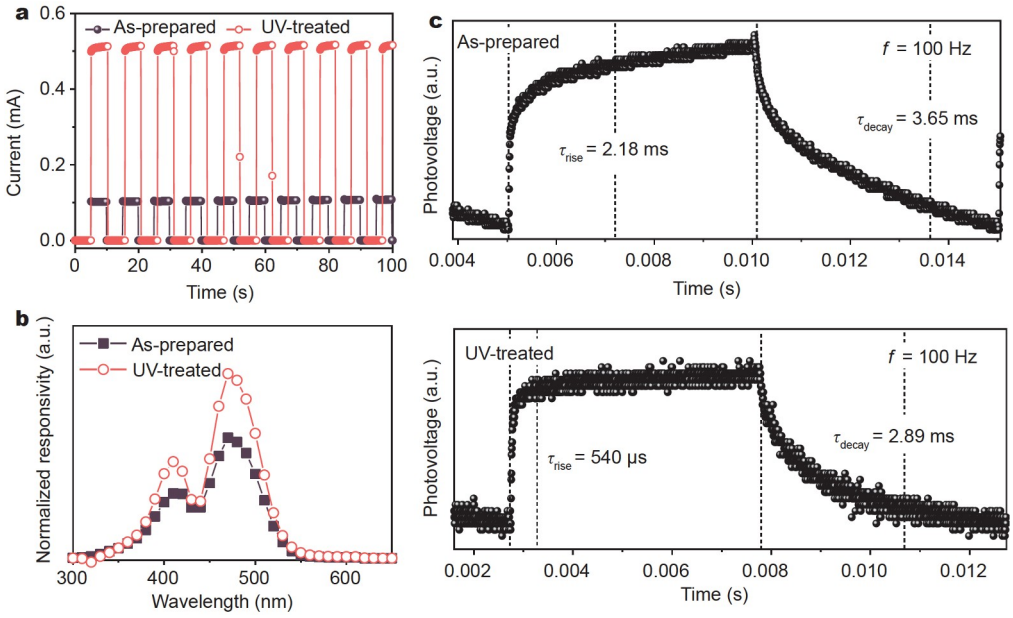

Figure 5 (a) *I-T* curves, (b) spectral photoresponse performance and (c) enlarged transient photoresponse curves of the as-prepared and UV-treated photodetectors with the structure of FTO/$Cs_2AgBiBr_6$/TiO_2/Au.

ing trend after UV treatment. These results further demonstrate that the approach of UV-induced treatment could effectively regulate the photoresponse performance of the $Cs_2AgBiBr_6$-based all-inorganic photodetectors, especially the light current and response speed, regardless of the specific device structure.

CONCLUSIONS

In summary, we investigated an UV-induced regulation of photoresponse performance for the $Cs_2AgBiBr_6$-based perovskite all-inorganic photodetectors. The devices exhibit favorable stability under UV illumination. Satisfyingly, it is found that the light current of the device with the structure of FTO/$Cs_2AgBiBr_6$/Au presents an increasing tendency with prolonged UV soaking treatment. Particularly, it is remarkably boosted from ~1.0×10^{-5} to ~1.5×10^{-4} A after UV soaking for 8 h. Furthermore, it is proved that the UV treatment can effectively modulate the rising and falling edges of the photoresponse curves. In this case, the rise/decay time of the device is significantly improved from 55.9/30.1 μs to 1.1/0.34 μs, which indicates that the response speed of the $Cs_2AgBiBr_6$-based perovskite photodetectors can be efficiently regulated by controlling the time for UV soaking. Besides, the −3 dB bandwidth increases from 5 to 20 kHz while the LDR is extended from 60 to 87 dB with UV treatment. Moreover, similar results are obtained from the $Cs_2AgBiBr_6$-based all-inorganic photodetectors with other structures, i.e., FTO/$Cs_2AgBiBr_6$/TiO_2/Au, FTO/TiO_2/$Cs_2AgBiBr_6$/Au and FTO/TiO_2/$Cs_2AgBiBr_6$/CuSCN/Au, indicating the universality of the approach of UV-induced regulation for photoresponse performance improvement. According to the characterization results, the UV-treated $Cs_2AgBiBr_6$ films present no obvious changes on surface morphology, element distribution and phase structure. The reason for the increased I_{light} and enhanced response speed is attributed to the improved electrical properties of the devices after UV illumination. From the EIS spectra, it is found that the series resistance of the device exhibits a decreasing trend after UV treatment, which is beneficial to the response speed improvement. This work demonstrates the positive role of UV light for perovskite devices and reveals an effective method to improve the photoresponse performance of the $Cs_2AgBiBr_6$-based all-inorganic photodetectors.

Received 13 April 2021; accepted 18 June 2021; published online 19 August 2021

1 Dong Q, Fang Y, Shao Y, *et al.* Electron-hole diffusion lengths > 175 μm in solution-grown $CH_3NH_3PbI_3$ single crystals. Science, 2015, 347: 967–970
2 Stranks SD, Eperon GE, Grancini G, *et al.* Electron-hole diffusion lengths exceeding 1 micrometer in an organometal trihalide perovskite absorber. Science, 2013, 342: 341–344
3 Kojima A, Teshima K, Shirai Y, *et al.* Organometal halide perovskites as visible-light sensitizers for photovoltaic cells. J Am Chem Soc, 2009, 131: 6050–6051
4 Wang S, Yousefi Amin AA, Wu L, *et al.* Perovskite nanocrystals: Synthesis, stability, and optoelectronic applications. Small Struct, 2021, 2: 2000124
5 Jeon NJ, Na H, Jung EH, *et al.* A fluorene-terminated hole-transporting material for highly efficient and stable perovskite solar cells. Nat Energy, 2018, 3: 682–689
6 Yang WS, Park BW, Jung EH, *et al.* Iodide management in formamidinium-lead-halide–based perovskite layers for efficient solar cells. Science, 2017, 356: 1376–1379
7 Cho H, Jeong SH, Park MH, *et al.* Overcoming the electroluminescence efficiency limitations of perovskite light-emitting diodes. Science, 2015, 350: 1222–1225
8 Lin K, Xing J, Quan LN, *et al.* Perovskite light-emitting diodes with external quantum efficiency exceeding 20 per cent. Nature, 2018, 562: 245–248
9 Cen G, Liu Y, Zhao C, *et al.* Atomic-layer deposition-assisted double-side interfacial engineering for high-performance flexible and stable $CsPbBr_3$ perovskite photodetectors toward visible light communication applications. Small, 2019, 15: 1902135
10 Yan G, Jiang B, Yuan Y, *et al.* Importance of Bi–O bonds at the

$Cs_2AgBiBr_6$ double-perovskite/substrate interface for crystal quality and photoelectric performance. ACS Appl Mater Interfaces, 2020, 12: 6064–6073
11 Liu CK, Loi HL, Cao J, *et al.* High-performance quasi-2D perovskite/single-walled carbon nanotube phototransistors for low-cost and sensitive broadband photodetection. Small Struct, 2020, 2: 2000084
12 Leijtens T, Eperon GE, Pathak S, *et al.* Overcoming ultraviolet light instability of sensitized TiO_2 with meso-superstructured organometal tri-halide perovskite solar cells. Nat Commun, 2013, 4: 2885
13 Aristidou N, Sanchez-Molina I, Chotchuangchutchaval T, *et al.* The role of oxygen in the degradation of methylammonium lead trihalide perovskite photoactive layers. Angew Chem Int Ed, 2015, 54: 8208–8212
14 Chen W, Chen H, Xu G, *et al.* Precise control of crystal growth for highly efficient $CsPbI_2Br$ perovskite solar cells. Joule, 2019, 3: 191–204
15 Zeng J, Zhou H, Liu R, *et al.* Combination of solution-phase process and halide exchange for all-inorganic, highly stable $CsPbBr_3$ perovskite nanowire photodetector. Sci China Mater, 2018, 62: 65–73
16 Wang P, Cai F, Yang L, *et al.* Eliminating light-soaking instability in planar heterojunction perovskite solar cells by interfacial modifications. ACS Appl Mater Interfaces, 2018, 10: 33144–33152
17 Wang K, Jin Z, Liang L, *et al.* Chlorine doping for black γ-$CsPbI_3$ solar cells with stabilized efficiency beyond 16%. Nano Energy, 2019, 58: 175–182
18 Zhao Y, Li C, Shen L. Recent advances on organic-inorganic hybrid perovskite photodetectors with fast response. InfoMat, 2019, 1: 164–182
19 Lei LZ, Shi ZF, Li Y, *et al.* High-efficiency and air-stable photodetectors based on lead-free double perovskite $Cs_2AgBiBr_6$ thin films. J Mater Chem C, 2018, 6: 7982–7988
20 Tang Y, Liang M, Chang B, *et al.* Lead-free double halide perovskite Cs_3BiBr_6 with well-defined crystal structure and high thermal stability for optoelectronics. J Mater Chem C, 2019, 7: 3369–3374
21 Luo J, Li S, Wu H, *et al.* $Cs_2AgInCl_6$ double perovskite single crystals: Parity forbidden transitions and their application for sensitive and fast UV photodetectors. ACS Photonics, 2017, 5: 398–405
22 Wu C, Du B, Luo W, *et al.* Highly efficient and stable self-powered ultraviolet and deep-blue photodetector based on $Cs_2AgBiBr_6/SnO_2$ heterojunction. Adv Opt Mater, 2018, 6: 1800811
23 Yang J, Bao C, Ning W, *et al.* Stable, high-sensitivity and fast-response photodetectors based on lead-free $Cs_2AgBiBr_6$ double perovskite films. Adv Opt Mater, 2019, 7: 1801732
24 Niezgoda JS, Foley BJ, Chen AZ, *et al.* Improved charge collection in highly efficient $CsPbBrI_2$ solar cells with light-induced dealloying. ACS Energy Lett, 2017, 2: 1043–1049
25 Xue J, Yang D, Cai B, *et al.* Photon-induced reversible phase transition in $CsPbBr_3$ perovskite. Adv Funct Mater, 2019, 29: 1807922
26 You P, Li G, Tang G, *et al.* Ultrafast laser-annealing of perovskite films for efficient perovskite solar cells. Energy Environ Sci, 2020, 13: 1187–1196
27 Yuan Y, Ji Z, Yan G, *et al.* TiO_2 electron transport bilayer for all-inorganic perovskite photodetectors with remarkably improved UV stability toward imaging applications. J Mater Sci Tech, 2021, 75: 39–47
28 Yuan Y, Zhang L, Yan G, *et al.* Significantly enhanced detectivity of CIGS broadband high-speed photodetectors by grain size control and ALD-Al_2O_3 interfacial-layer modification. ACS Appl Mater Interfaces, 2019, 11: 20157–20166
29 Wu C, Zhang Q, Liu Y, *et al.* The dawn of lead-free perovskite solar cell: Highly stable double perovskite $Cs_2AgBiBr_6$ film. Adv Sci, 2018, 5: 1700759
30 Zhao C, Chen B, Qiao X, *et al.* Revealing underlying processes involved in light soaking effects and hysteresis phenomena in perovskite solar cells. Adv Energy Mater, 2015, 5: 1500279
31 Hu J, Gottesman R, Gouda L, *et al.* Photovoltage behavior in perovskite solar cells under light-soaking showing photoinduced interfacial changes. ACS Energy Lett, 2017, 2: 950–956
32 Deng X, Wen X, Zheng J, *et al.* Dynamic study of the light soaking effect on perovskite solar cells by *in-situ* photoluminescence microscopy. Nano Energy, 2018, 46: 356–364
33 Shao S, Abdu-Aguye M, Sherkar TS, *et al.* The effect of the microstructure on trap-assisted recombination and light soaking phenomenon in hybrid perovskite solar cells. Adv Funct Mater, 2016, 26: 8094–8102
34 Shao S, Abdu-Aguye M, Qiu L, *et al.* Elimination of the light soaking effect and performance enhancement in perovskite solar cells using a fullerene derivative. Energy Environ Sci, 2016, 9: 2444–2452
35 Tress W, Yavari M, Domanski K, *et al.* Interpretation and evolution of open-circuit voltage, recombination, ideality factor and subgap defect states during reversible light-soaking and irreversible degradation of perovskite solar cells. Energy Environ Sci, 2018, 11: 151–165
36 Yamada Y, Endo M, Wakamiya A, *et al.* Spontaneous defect annihilation in $CH_3NH_3PbI_3$ thin films at room temperature revealed by time-resolved photoluminescence spectroscopy. J Phys Chem Lett, 2015, 6: 482–486
37 Tian Y, Merdasa A, Unger E, *et al.* Enhanced organo-metal halide perovskite photoluminescence from nanosized defect-free crystallites and emitting sites. J Phys Chem Lett, 2015, 6: 4171–4177
38 Tian Y, Peter M, Unger E, *et al.* Mechanistic insights into perovskite photoluminescence enhancement: light curing with oxygen can boost yield thousandfold. Phys Chem Chem Phys, 2015, 17: 24978–24987
39 Chen S, Wen X, Huang S, *et al.* Light illumination induced photoluminescence enhancement and quenching in lead halide perovskite. Sol RRL, 2017, 1: 1600001
40 Hoke ET, Slotcavage DJ, Dohner ER, *et al.* Reversible photo-induced trap formation in mixed-halide hybrid perovskites for photovoltaics. Chem Sci, 2015, 6: 613–617
41 Lee SW, Kim S, Bae S, *et al.* UV degradation and recovery of perovskite solar cells. Sci Rep, 2016, 6: 38150
42 Zhang Z, Cao D, Huang Z, *et al.* Gamma-ray detection using Bi-poor $Cs_2AgBiBr_6$ double perovskite single crystals. Adv Opt Mater, 2021, 9: 2001575
43 Liang F, Jiang J, Zhao Y, *et al.* Fabrication of $MAPbBr_3$ single crystal p-n photodiode and n-p-n phototriode for sensitive light detection application. Adv Funct Mater, 2020, 30: 2001033

Acknowledgements This work was supported by the National Natural Science Foundation of China (51772135 and 52002148), the Ministry of Education of China (6141A02022516), the Fundamental Research Funds for the Central Universities (11619103) and Guangdong Basic and Applied Basic Research Foundation (2020A1515011377). Yuan Y and Yan G thank the support from China and Germany Postdoctoral Exchange Program. Fan HJ thanks the financial support from Agency for Science, Technology, and Research (A*STAR), Singapore by the AME Individual Research Grants (A1883c0004).

Author contributions Yuan Y proposed the idea, designed and engineered the device samples; Li Z and Jiang B performed the chemical experiments and the characterization; Yan G proposed the idea, analyzed the data and wrote the paper; Liang Z guided the characterization and data analysis; Fan HJ provided guidance and suggestions; this work was guided and supported by Mai W. All authors contributed to the general discussion.

Conflict of interest The authors declare no conflict of interest.

Supplementary information Supporting data are available in the online version of the paper.

Ye Yuan received his BSc degree in optical information science and technology in 2013 and PhD degree in materials physics and chemistry in 2018 from Sun Yat-sen University (SYSU). He is now an assistant research fellow at the School of Physics, SYSU. His research interests are thin film photoelectric materials and devices, especially heterojunction photodetectors and solar cells.

Genghua Yan received her BSc degree in applied physics from the Central South University in 2013 and DE degree in materials physics and chemistry from SYSU in 2018. She joined the College of Science and Engineering, Jinan University as a postdoctor in the middle of 2018. She is now an assistant research fellow at the School of Physics, SYSU. Her main research interest focuses on advanced thin film materials and photoelectric devices.

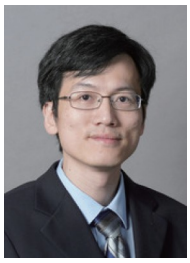

Wenjie Mai is a professor as well as the head of the Deparment of Physics, Jinan University. He received his BSc degree from Peking University in 2002 and PhD degree from Georgia Institute of Technology (GIT) in 2009. He joined Jinan University in 2009. He was a visiting fellow at GIT from 2012 to 2013. His research area includes photoelectric materials, energy materials and the related flexible devices. His research currently focuses on supercapacitors, photodetectors and solar cells.

利用紫外光浸泡效应提升$Cs_2AgBiBr_6$全无机钙钛矿光电探测器响应速度及光电流

袁野[1,2], 颜庚骅[1,2*], 李卓伟[2], 江邦齐[2], 梁宗存[1], 范红金[4], 麦文杰[2,3*]

摘要 目前已报道的$Cs_2AgBiBr_6$光电探测器的响应速度在毫秒到纳秒量级宽度区间变化, 随机性强, 但原因尚不明确, 新的响应速度调控方法也鲜有报道. 此外, 在传统观念中, 紫外光通常被认为对钙钛矿器件存在有害作用, 会使器件性能衰减. 在本工作中, 我们证明了在不减小器件面积的情况下, FTO/$Cs_2AgBiBr_6$/Au结构光电探测器的响应速度可以利用紫外光浸泡效应实现有效调控. 特别是下降时间可以从30.1 μs有效调控到340 ns, 且器件的−3 dB带宽可从5 kHz扩展至20 kHz. 值得一提的是, 紫外光浸泡处理后, 器件光电流显著提升了15倍. 此外, 我们还进一步证明了紫外光浸泡处理方法对FTO/TiO_2/$Cs_2AgBiBr_6$/Au、FTO/$Cs_2AgBiBr_6$/TiO_2/Au和FTO/TiO_2/$Cs_2AgBiBr_6$/CuSCN/Au结构的$Cs_2AgBiBr_6$基器件同样有效. 本工作为提高$Cs_2AgBiBr_6$全无机钙钛矿光电探测器响应速度和光电流提供了新的方法和思路.